10612 *Macromolecules* **2010**, *43*, 10612–10620
DOI: 10.1021/ma102296r

Macromolecules
ARTICLE

Self-Assembly of Lamellar Microphases in Linear Gradient Copolymer Melts

Nicholas B. Tito, Scott T. Milner, and Jane E. G. Lipson*

Department of Chemistry, Dartmouth College, Hanover, New Hampshire 03755, United States

Received October 6, 2010

ABSTRACT: We investigate lamellar microphases in linear gradient copolymer melts by a combination of techniques, including numerical solutions of self-consistent field equations, scaling theory, and analysis of the strong-segregation limit. In particular, we construct a Flory theory to predict the scaling of the equilibrium lamellar width L_{eq} as a function of comonomer incompatibility measured by χN. The Flory theory balances chain stretching with increased monomer repulsive interactions resulting from conformational fluctuations about a state of uniformly stretched chains, that obtains in the strong-segregation limit. We find $L_{eq}/R_g \sim (\chi N)^{1/6}$, which agrees well with numerical results. Remarkably, this is the same result as for symmetric diblock copolymers, although for quite different physical reasons.

Introduction

Recent advances in living polymerization techniques have allowed for the synthesis of unique copolymers with controlled monomeric sequences.[1−3] Among these new materials are the so-called "gradient copolymers", which are copolymers composed of two monomeric species with concentration varying smoothly along the chain.[4] "Linear" gradient copolymers, in which the comonomer concentration varies linearly along the entire length of the chain, have received particular experimental attention due to their high potential for commercial application.[5−11]

Copolymer melts composed of immiscible A and B monomers exhibit the formation of "microphases", or distinct segregated phases at the microscopic scale. Symmetric diblock copolymers in particular have been thoroughly studied both experimentally and theoretically, and are seen to self-assemble into layer-like "lamellar" microphases.[12−16] In these phases, as the two species become increasingly incompatible the A−B junctions are confined into relatively narrow interfaces, which separate domains composed of the chains' A- and B-blocks. Unfavorable A−B contact is restricted to the surfaces between each layer, at the expense of reduced chain conformational entropy.

Melts of linear gradient copolymers exhibit a rather different lamellar microphase structure. The smooth variation of monomer concentration along the chain means that there is no distinguished point that separates A- and B-rich portions of the chain, as for diblocks. This architecture leads to lamellae in which the A−B concentration profile varies smoothly, nearly sinusoidally, without any indication of a sharp interface between A- and B-rich domains.

Theoretical studies of gradient copolymers have modeled their microphase segregation and phase behavior using self-consistent field theories, such as in bulk melts[17−21] and at interfaces between immiscible homopolymer blends.[22] But little work has been done to construct analytical models of their microphase behavior. A scaling theory for a thermally controlled chain free-end "exclusion zone" in linear gradient copolymer melt brushes has been formulated by Pickett;[23] however, no such tool has been developed to predict lamellar width in bulk ordered phases of the copolymers, which is the primary objective of this work.

Previous research has shown that the widths of symmetric diblock copolymer lamellae are dependent upon the energy of interaction between the A and B monomers as well as the chain lengths.[24−26] The scaling theory is of the form

$$\frac{L_{eq}}{R_g} \sim (\chi N)^{1/6} \tag{1}$$

where L_{eq} is the width of one lamella (that which minimizes the free energy per chain), R_g is the chains' average radius of gyration (defined as $a(N/6)^{1/2}$), a is the width of one monomer (A and B assumed to be equal), χ is a dimensionless Flory−Huggins A−B monomer interaction parameter, and N is the number of segments composing the chain. A similar scaling relation for linear gradient copolymer lamellae has been previously suggested by Lefebvre et al.[19] based on numerical self-consistent field calculations.

In this paper we show that the competition between hydrostatic pressure and comonomer interaction drives lamellar formation in linear gradient copolymer melts. These factors operate in a fundamentally different way from their role in diblock copolymer melt lamellae. We explore the behavior of linear gradient copolymer melt lamellae as a function of χN using numerical solutions of self-consistent field equations, which allow us to determine the equilibrium free energy per chain, lamellar phase widths, and monomer concentration and pressure profiles. Then, we derive a scaling theory for L_{eq} in terms of χ and N by considering the enthalpic and entropic contributions to chain free energy at the molecular scale. Our surprising conclusion is that the scaling expression takes an identical form to that for symmetric diblock copolymer lamellae, albeit for quite different physical reasons.

Partition Function and Free Energy

In this section we develop an expression for the free energy per chain in a copolymeric system. This is done by decoupling segment interactions in the associated multichain partition function into interactions with conjugate chemical fields, and then applying the mean-field approximation. We begin by defining the

*To whom correspondence should be addressed. E-mail: Jane.E.G.Lipson@Dartmouth.edu.

 Published on Web 12/03/2010

partition function as the product over all chains J in the system, indexed by j, of the path integral for each chain configuration

$$Z = \frac{1}{J!}\left[\prod_{j=1}^{J}\int DS(t)\mathrm{e}^{-\beta\varepsilon_S}\mathrm{e}^{-\beta\varepsilon_H}\right]\prod_{\mathbf{r}}\delta(\hat{\phi}_\mathrm{A}(\mathbf{r})+\hat{\phi}_\mathrm{B}(\mathbf{r})-1) \tag{2}$$

where $S(t)$ are spacecurves with continuous parameter t ranging from 0 to N representing possible chain conformations, $\mathbf{r}$ is a real-space coordinate, and $\delta(x)$ is the Dirac delta function applied to argument x. The inverse factor of $J!$ accounts for the indistinguishability of the J chains (i.e., we assume they are statistically identical). The monomer volume fraction operator for component i, $\hat{\phi}_i(\mathbf{r})$, returns the number of monomers of type i in the unit volume a^3 centered at $\mathbf{r}$, divided by the melt density ρ (which we take to be unity per a^3). These are

$$\hat{\phi}_\mathrm{A}(\mathbf{r}) = \frac{1}{a^3\rho}\sum_{j=1}^{J}\int_0^N \mathrm{d}t\,\delta(S_j(t)-\mathbf{r})g(t) \tag{3}$$

$$\hat{\phi}_\mathrm{B}(\mathbf{r}) = \frac{1}{a^3\rho}\sum_{j=1}^{J}\int_0^N \mathrm{d}t\,\delta(S_j(t)-\mathbf{r})(1-g(t)) \tag{4}$$

Here $g(t)$ is the probability of finding a type A monomer at position t on the chain. For the linear gradient copolymer architecture, $g(t)$ is given by

$$g(t) = 1-\frac{t}{N} \tag{5}$$

In eq 2, ε_S is the stretching energy of a chain with conformation $S(t)$, given by

$$\varepsilon_S = \frac{3k_\mathrm{B}T}{2a^2}\int_0^N \mathrm{d}t\left|\frac{\mathrm{d}S(t)}{\mathrm{d}t}\right|^2 \tag{6}$$

Likewise, ε_H represents the sum of all A-B monomer interactions in the system, and is given by

$$\varepsilon_H = -\frac{1}{4}k_\mathrm{B}T\rho\chi\int \mathrm{d}^3\mathbf{r}\,(\hat{\phi}_\mathrm{A}(\mathbf{r})-\hat{\phi}_\mathrm{B}(\mathbf{r}))^2 \tag{7}$$

The form we use is equivalent to the standard Flory−Huggins incompressible fluid expression for internal energy change on mixing, with the reference state taken as a uniform copolymer melt with $\hat{\phi}_\mathrm{A}(\mathbf{r}) = \hat{\phi}_\mathrm{B}(\mathbf{r}) = {}^1/_2$ at all $\mathbf{r}$. This is seen by the equality

$$\chi\hat{\phi}_\mathrm{A}(\mathbf{r})\hat{\phi}_\mathrm{B}(\mathbf{r}) = \frac{1}{4}\chi\,[(\hat{\phi}_\mathrm{A}(\mathbf{r})+\hat{\phi}_\mathrm{B}(\mathbf{r}))^2-(\hat{\phi}_\mathrm{A}(\mathbf{r})-\hat{\phi}_\mathrm{B}(\mathbf{r}))^2] \tag{8}$$

The product of Dirac delta functionals over space in eq 2 constrains the partition function to only include system configurations that exhibit uniform melt volume fraction of unity, so the term $(\hat{\phi}_\mathrm{A}(\mathbf{r})+\hat{\phi}_\mathrm{B}(\mathbf{r}))^2$ in eq 8 is ultimately equal to unity.

By decoupling the particle interactions into single particles interacting with conjugate chemical potential fields,[15] the multi-chain partition function becomes

$$Z = \frac{1}{J!}\int DV(\mathbf{r})\mathrm{e}^{\rho\int \mathrm{d}^3\mathbf{r}V(\mathbf{r})} \times\int DW(\mathbf{r})\mathrm{e}^{-(1/\chi)\rho\int \mathrm{d}^3\mathbf{r}W(\mathbf{r})^2}(Z_1[V(\mathbf{r}),W(\mathbf{r})])^J \tag{9}$$

The field $V(\mathbf{r})$ can be identified as proportional to the hydrostatic pressure field conjugate to the overall monomer density. Likewise, the field $W(\mathbf{r})$ is related to the exchange chemical potential for the A-B monomer concentration difference. The single-chain partition function, $Z_1[V(\mathbf{r}),W(\mathbf{r})]$, can be written with the aid of the monomer volume fraction operators, eqs 3 and 4, as

$$Z_1[V(\mathbf{r}),W(\mathbf{r})] = \int DS(t)\mathrm{e}^{-\int_0^N \mathrm{d}t\left[\frac{3}{2a^2}\left|\frac{\mathrm{d}S(t)}{\mathrm{d}t}\right|^2+V(S(t))+W(S(t))(1-2g(t))\right]} \tag{10}$$

The single-chain partition function is of Gaussian form and can be computed explicitly, for given potential field configurations $V(\mathbf{r})$ and $W(\mathbf{r})$, by methods we describe in the next section.

The self-consistent mean fields $V^*(\mathbf{r})$ and $W^*(\mathbf{r})$ are obtained by extremizing the integrand of eq 9 via steepest descent.[15] This leads to the self-consistent equations

$$\langle\hat{\phi}_\mathrm{A}(\mathbf{r})+\hat{\phi}_\mathrm{B}(\mathbf{r})\rangle = 1 \tag{11}$$

$$W^*(\mathbf{r}) = \frac{1}{2}\chi\,\langle\hat{\phi}_\mathrm{A}(\mathbf{r})-\hat{\phi}_\mathrm{B}(\mathbf{r})\rangle \tag{12}$$

in which the angle-bracketed quantities represent averages over the single-chain partition function at $\mathbf{r}$. The field $V^*(\mathbf{r})$ is chosen to satisfy eq 11, i.e., such that the uniform melt density condition is met. The field $W^*(\mathbf{r})$ is interpreted as a "monomer exchange" chemical potential. It is half the change in internal energy of the system upon substituting a type B monomer in place of a type A monomer at position $\mathbf{r}$ in the system. The strength of the potential is scaled by how B-like the monomer is, measured by $(1-2g(t))$ as seen in the single-chain partition function, eq 10. See Appendix A for a thermodynamic derivation of this form.

The Helmholtz free energy of the system is obtained from the standard relation

$$\frac{F}{k_\mathrm{B}T} = -\ln Z \tag{13}$$

Applying eq 13 to the partition function we obtained in eq 9 allows us to obtain the free energy per chain

$$\frac{F}{Jk_\mathrm{B}T} = \frac{F_1}{k_\mathrm{B}T} = -\ln Z_1[V^*(\mathbf{r}),W^*(\mathbf{r})]+\ln J -\frac{\rho}{J}\int \mathrm{d}^3\mathbf{r}\left[V^*(\mathbf{r})-\frac{1}{4}\chi\,(\hat{\phi}_\mathrm{A}(\mathbf{r})-\hat{\phi}_\mathrm{B}(\mathbf{r}))^2\right] \tag{14}$$

Thus, the free energy per chain is given by the natural logarithm of the single-chain partition function, with three correction factors. The first accounts for indistinguishability of chains. The second serves to remove the energy contributed from the hydrostatic pressure field $V^*(\mathbf{r})$ (which was introduced simply to enforce uniform monomer density, and so does no work on the system). The third correction corrects for double counting of the monomer−monomer interaction energy, adding back half of the chain's interaction energy with the monomer exchange potential field. (Each chain technically only bears half of its interaction energy; other chains in the system collectively hold the other half.)

Self-Consistent Field Lattice Model

Here we use a lattice model to study the equilibrium conformations of chains in linear gradient copolymer melt lamellae. The Scheutjens−Fleer[27,28] lattice version of self-consistent field theory for copolymer chains, similar to the approach of Lefebvre et al.,[19] approximates the single-chain partition function in eq 10 and obtains the self-consistent fields V^* and W^* for a specified lamellar width L and χN.

A three-dimensional simple cubic lattice comprised of sites of volume a^3 is defined, with one coordinate axis m aligned perpendicular to the orientation of the lamellae. Each lattice "layer" is indexed by $m = 1, 2, ..., M$, beginning at the center of an A-rich lamella and ending at the center of an adjacent B-rich lamella, so that $aM = L$ is the prescribed width of one lamella (half the width of a full lamellar period).[29] The volume of the lattice is just sufficient to contain J chains each with N segments (we assume that A and B monomers have the same volume of a^3). Thus, the number of sites per layer $\mathcal{A}$ satisfies the relation $\mathcal{A}M = NJ$ As the lamellae are compositionally homogeneous in the dimensions parallel to their orientation, our calculations are only concerned with fields and properties in the perpendicular m dimension.

The lattice model uses the method of chain propagators in self-consistent fields[15] to compute a statistical distribution of conformations for a linear gradient copolymer. The chain has a composition function of

$$g(n) = 1 - \frac{n-1}{N-1} \tag{15}$$

where n is a segment index running from 1 to N and $g(n)$ is the probability that segment n is of type A. Boltzmann weights for all chain conformations in the lattice are generated by two random-walking propagators, each interpreted as starting from one of the two ends of the chain.[15,30] The mapping of walker step i (which also runs from 1 to N) to real chain segment n follows

$$n(i) = \begin{cases} i & \text{for walker 1} \\ N - i + 1 & \text{for walker 2} \end{cases} \tag{16}$$

The probabilities of finding the walkers at layer m on step i are given by $P_1(m,i)$ and $P_2(m,i)$. The distributions follow a modified diffusion equation developed by Edwards[31] and Helfand.[24] This is written for both walkers in a discretized form for a simple cubic lattice as

$$P(m,i) = \mathrm{e}^{-V(m)}\mathrm{e}^{-w(m,i)}\left[\frac{1}{6}P(m-1,i-1) + \frac{4}{6}P(m,i-1) + \frac{1}{6}P(m+1,i-1)\right] \tag{17}$$

The walk is biased by both the hydrostatic pressure and monomer exchange potential fields, incorporated here as $V(m)$ and $W(m)$, analogously to their role in the decoupled single-chain partition function obtained in the previous section. The local interaction of walker step i with the monomer exchange field takes the same form as in eq 10

$$w(m,i) = \frac{1}{2}\chi\,[\phi_A(m) - \phi_B(m)][1 - 2g(n(i))] \tag{18}$$

where $\phi_A(m) = 1 - \phi_B(m)$ are the volume fractions of monomer types A and B at layer m. The boundary conditions used in eq 17 for lamellar microphases are as follows. First, the walkers start at each layer m with the Boltzmann weight for placing monomer 1 (for P_1) or N (for P_2) at that layer:

$$P_1(m,1) = \mathrm{e}^{-V(m)}\mathrm{e}^{-w(m,1)} \tag{19}$$

$$P_2(m,1) = \mathrm{e}^{-V(m)}\mathrm{e}^{-w(m,1)} \tag{20}$$

Second, reflecting boundary layers $m = 0$ and $m = M + 1$ are included at either side of the lattice,

$$P(0,i) = P(1,i) \quad \text{and} \quad P(M+1,i) = P(M,i) \tag{21}$$

The sum of Boltzmann weights for chain conformations in which real chain segment n resides at layer m is given by

$$Q(m,n) = P_1(m,n)P_2(m,N-n+1)\mathrm{e}^{V(m)}\mathrm{e}^{w(m,n)} \tag{22}$$

(Both P_1 and P_2 contain the Boltzmann weight for placement of segment n at layer m; the two exponential terms in eq 22 correct for this by negating one of them.) The *probability* that chain segment n is at layer m is therefore

$$p(m,n) = \frac{Q(m,n)}{\sum_{m=1}^{M} Q(m,n)} = \mathcal{A}\frac{Q(m,n)}{Z_1(n)} \tag{23}$$

Here the definition of the single-chain partition function for the lattice system has been introduced as the sum of Boltzmann weights for chain conformations that have their nth segment located at *any* m,

$$Z_1(n) = \mathcal{A}\sum_{m=1}^{M} Q(m,n) \tag{24}$$

The sum of $Q(m,n)$ must be multiplied by the number of sites per lattice layer, $\mathcal{A}$, to account for all possible locations in each m at which segment n can be located. The numerical value of the partition function is independent of the segment n chosen to calculate it for a given system.

The fraction of lattice sites at layer m occupied by monomers is found by first obtaining the total number of monomers at layer m, $J\Sigma_n p(m,n)$, and then dividing by the number of sites per layer, $\mathcal{A}$. This is equivalently written as

$$\phi(m) = M\frac{\sum_{n=1}^{N} Q(m,n)}{\sum_{m=1}^{M}\sum_{n=1}^{N} Q(m,n)} \tag{25}$$

The contribution from only type A or B monomers is given by the probability that each segment is of the respective type

$$\phi_A(m) = M\frac{\sum_{n=1}^{N} Q(m,n)g(n)}{\sum_{m=1}^{M}\sum_{n=1}^{N} Q(m,n)} \tag{26}$$

$$\phi_B(m) = M\frac{\sum_{n=1}^{N} Q(m,n)(1-g(n))}{\sum_{m=1}^{M}\sum_{n=1}^{N} Q(m,n)} \tag{27}$$

Equations 25−27 form a set of $2M$ equations in $2M$ unknowns which are solved self-consistently to obtain the fields $V^*(m)$ and $\phi_A(m)$ for a given χ, N, and M. Incompressibility is enforced by the constraint that $\phi(m) = 1$ for all m.

The free energy per chain for the lattice system is obtained by adaptation of eq 14. The volume integral over $d^3\mathbf{r}$ is replaced by $\mathcal{A}a^3$ times a sum over the m layers. The density ρ of the system is one monomer per lattice site, $1/a^3$. The free energy per chain is thus

$$\frac{F_1}{k_B T} = -\ln Z_1 + \ln J - \frac{N}{M}\sum_{m=1}^{M}\left[V^*(m) - \frac{1}{4}\chi\,(\phi_A(m) - \phi_B(m))^2\right] \tag{28}$$

Note that a uniform shift of the hydrostatic pressure field $V(m)$ by an additive constant δV (i.e., $V'(m) = V(m) + \delta V$) does not influence the lattice layer volume fractions (eqs 25−27) or single-chain free energy. These properties are also independent of the number of chains J in the system, as each chain has identical statistical behavior (recall that the chains interact only with the two mean fields and are not influenced by interactions with each other).

Numerical Results

Numerical self-consistent field calculations were performed at various L for a series of fixed χN. From these we find the optimum lamellar width L_{eq} that minimizes the free energy per chain, eq 28. The degree of polymerization is fixed at $N = 400$ and the lattice cell volume is set as $a^3 = 1$. Plots of the free energy per chain as a function of $2L/R_g$ (the width of one full lamellar period divided by R_g) for calculations at several χN are shown in Figure 1. Each curve has a minimum located at some $2L/R_g$, which we refer to as $2L_{eq}/R_g$ (i.e., $2aM_{eq}/R_g$). The dependence of $2L_{eq}/R_g$ on χN is evident from the log−log plot in Figure 2. A linear fit of this data yields

$$\frac{2L_{eq}}{R_g} \sim (\chi N)^{0.216 \pm 0.004} \tag{29}$$

Our results are in excellent agreement with previous self-consistent field calculations for linear gradient copolymer melt lamellae by Lefebvre et al.,[19] as is apparent from comparison of their predictions of equilibrium lamellar period as a function of χN included in Figure 2. This power-law scaling is also quite similar to that found by Shull[26] for diblock copolymer melt lamellae using numerical self-consistent field calculations.

Composition Profiles. To understand more deeply the origin of the power-law scaling of lamellar width versus χN, we begin by examining the systematic variation of the composition profile in lamellar phases of linear gradient copolymers as χN increases. Figure 3 presents profiles for the A monomer volume fraction as a function of scaled distance $m_{rel} = (m-1)/(M_{eq}-1)$ for a variety of χN values (80, 160, 360). As χN increases, the initially sinusoidal composition profiles sharpen, gradually approaching a "sawtooth" pattern which can be written as a function of layer index as

$$\phi_A^o(m) = 1 - \frac{m-1}{M_{eq}-1} \tag{30}$$

This limiting sawtooth composition profile corresponds to uniformly stretched chains. We can see that the composition profile in the limit of large χN should approach uniformly stretched chains by the following argument. When the repulsive interaction between A and B monomers becomes large, maximization of like−like monomer contact dominates the free energy. Uniformly stretched parallel chains results in every portion of every chain being surrounded by material from other chains at the same average composition. This is the best separation of A from B that can be achieved for a linear gradient chain architecture.

Note that the A−B interaction energy per chain for a uniformly stretched state is *independent* of the degree of stretch. The above argument by itself cannot determine the lamellar period; for this, we must consider fluctuation corrections to the large-χN limit. The "rounding" of the tips of the teeth in the sawtooth profile, which evidently depends on χN, must be caused by fluctuations. We discuss the nature of these fluctuations, and how they give rise to the optimal lamellar width L_{eq} for a given value of χN, in the next section.

Profiles for *W*, *U*, and *V* Fields. Next, we examine the profiles of the self-consistent monomer exchange field $W^*(m)$, shown in

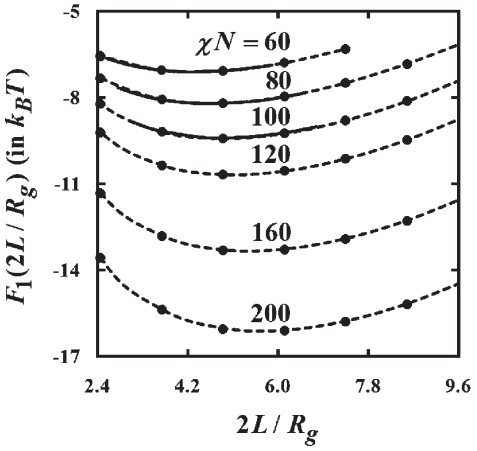

Figure 1. Free energy per chain, eq 28, vs lamellar period width relative to the radius of gyration, $2L/R_g$, for selected χN. Points are values from self-consistent field calculations. Dashed lines are fits of the results. Solid lines are self-consistent field calculations for $\chi N = 60$, 80, and 100 from Lefebvre et al.[19] (vertically shifted for ease of comparison with our results).

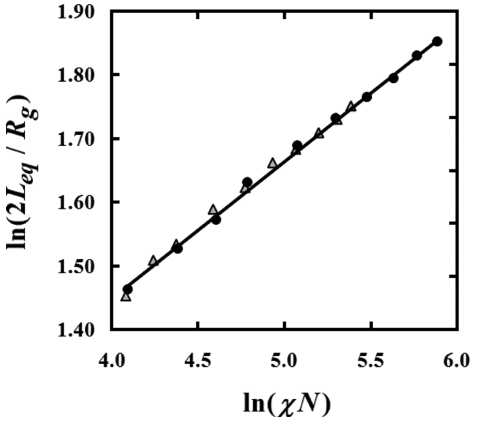

Figure 2. The log−log plot of $2L_{eq}/R_g$ versus χN. Black circles are our self-consistent field calculations, and the solid line is linear fit with slope 0.216 ± 0.004. Gray triangles are self-consistent field calculations from Lefebvre et al.[19]

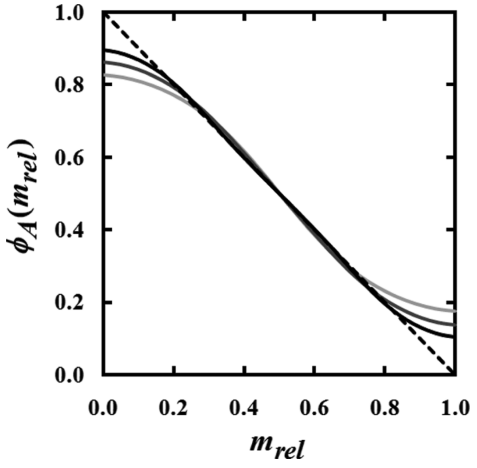

Figure 3. Monomer A volume fraction profiles for lamellae of optimum width L_{eq} at $\chi N = 80$, 160, and 360 (from lightest to darkest gray), plotted versus relative lattice layer coordinates $m_{rel} = (m-1)/(M_{eq}-1)$. Dashed line is expected profile in strongly stretched limit.

Figure 4. The exchange field acts oppositely on A and B monomers. Its influence on a monomer, n, is scaled by how "B-like" the monomer is via the scaling $(1 - 2g(n))$, as seen in eqs 10 and 18.

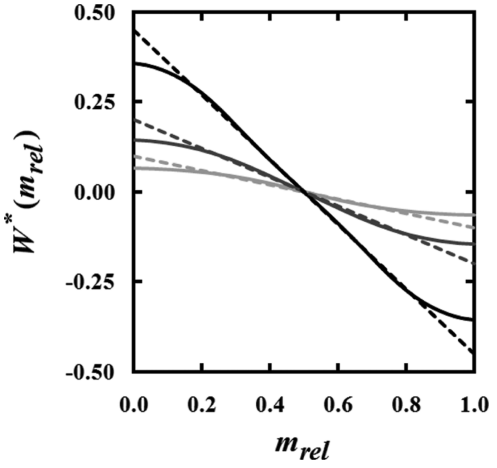

Figure 4. Profiles of the self-consistent monomer exchange potential fields $W^*(m)$ for lamellae of width L_{eq} at various χN. See the caption in Figure 3 for plot details.

The minimum at the center of the B-rich lamella pulls B-like monomers of the chains to the right-hand side of the image. Similarly, A-like monomers are pulled toward the left-hand side of the image by the maximum at the center of the A-rich lamella. Monomers with $g(n)$ near one-half are pulled only weakly in the corresponding direction. The net result is that the chains are stretched due to equal forces, driven by $W^*(m)$, pulling at their two ends. The strength of the potential, and thus the stretching force, increases as χN is raised.

It is illuminating to understand how $W^*(m)$ acts on a single chain by considering its "net" influence on the monomers located at each layer m. At equilibrium, the average composition of the $\mathcal{M}$ monomers located at lattice layer m is $\phi_A(m)$. The scaled influence of $W^*(m)$ on these monomers is therefore given (per monomer) by

$$W^*(m)(1-2\phi_A(m)) = -\frac{1}{2}\chi\,(\phi_A(m)-\phi_B(m))^2 \equiv 2U^*(m) \tag{31}$$

Plots of $U^*(m)$ are given in Figure 5. The minima at the edges of the image draw the two ends of the chains apart, toward the centers of the lamellae.

The hydrostatic pressure field $V^*(m)$, which acts on both monomer species equally, is seen in Figure 6. It pulls monomers back *inward* toward the center of the interfacial zone, into the less favorable mixed environment, so that the constant melt density is satisfied. Note that all profiles have been uniformly shifted vertically such that their minima are located at $V^*(m) = 0$, for visual convenience (recalling that the vertical position of the pressure field does not influence the single-chain free energy or chain propagator lattice statistics). The total field, $U^*(m) + V^*(m)$, is nearly a constant as seen in Figure 7. We work toward an understanding of this observation in the next section.

The self-consistent fields for the linear gradient copolymer lamellar phase stand in stark contrast to those found for symmetric diblock copolymers, indicating that although the scaling of the lamellar period with χN may be similar, the underlying physics in the two systems is quite different. For diblocks, A−B monomer repulsion serves to drive the junction points into narrow interfacial zones. The chain blocks are then pushed outward from the interface by hydrostatic pressure only, like back-to-back homopolymer melt brushes.[32] The $V^*(m)$ field is thus an inverted parabola with a maximum at the A−B interface. In contrast, for linear gradient copolymers the outward driving force on the more "pure" A-rich and B-rich ends of the chain away from the region where chain midpoints are found arises instead from the exchange chemical potential $W^*(m)$, i.e., from A−B repulsions. To maintain constant melt density, the hydrostatic pressure field $V^*(m)$ pulls the chains back inward toward the middle of the broad interfacial region.

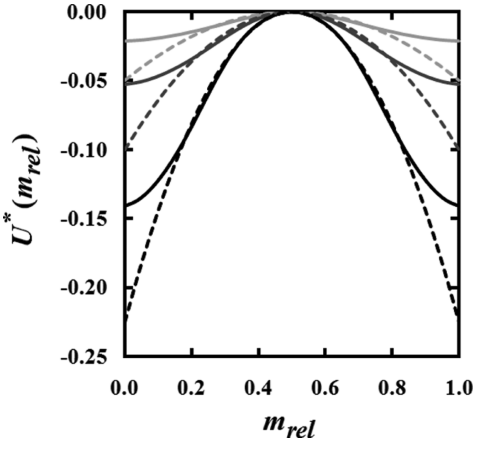

Figure 5. Profiles of the self-consistent $U^*(m)$ fields for lamellae of width L_{eq} at various χN. See the caption in Figure 3 for plot details.

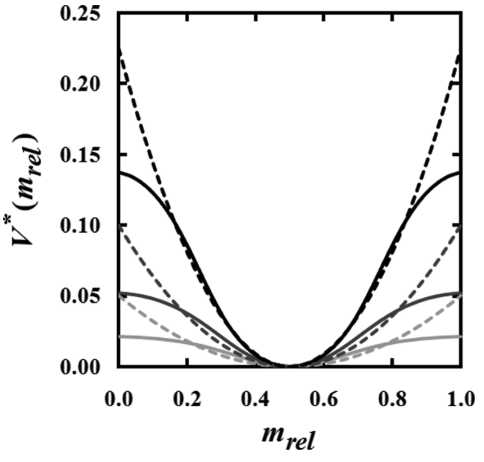

Figure 6. Profiles of the self-consistent hydrostatic pressure potential fields $V^*(m)$ for lamellae of width L_{eq} at various χN. See the caption in Figure 3 for plot details.

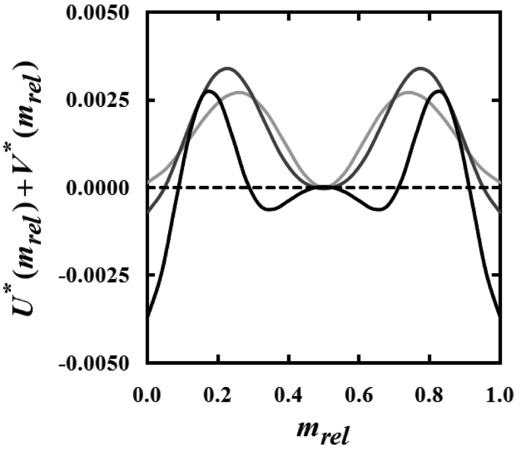

Figure 7. Profiles of the net self-consistent potential fields ($U^*(m) + V^*(m)$) for lamellae of width L_{eq} at various χN. See the caption in Figure 3 for plot details.

Strong-Stretching Limit for Linear Gradient Copolymers. In the high-χN limit, all chains are uniformly stretched along their entire length in order to maximize contact of like monomers. We show in this section that a constant total potential, $U(m) + V(m) = C$, is consistent with the scenario of uniformly stretched chains in mechanical equilibrium. We begin by developing the "equation of motion" for a single linear gradient copolymer chain in the lamellae.[32] In this "strong-stretching limit" only one chain conformation is contained in the single-chain partition function seen in eq 10: the uniformly stretched conformation $S^o(t)$. We have

$$Z_1^o[V^o(z), W^o(z)] = \mathrm{e}^{-\int_0^N \mathrm{d}t \left[\frac{3}{2a^2}\left|\frac{\mathrm{d}S^o(t)}{\mathrm{d}t}\right|^2 + V(S^o(t)) + W(S^o(t))(1-2g(t))\right]} \tag{32}$$

where z is a coordinate axis perpendicular to the lamellae (the continuum analogue of m), and $S^o(t)$ we redefine as the projection of the uniformly stretched chain conformation on the z-axis. Upon action minimization of the integrand in eq 32, we obtain the equation of motion for $S^o(t)$ as

$$\frac{3}{a^2}\frac{\mathrm{d}^2S^o(t)}{\mathrm{d}t^2} = \frac{\mathrm{d}V(z)}{\mathrm{d}z} + (1-2g(t))\frac{\mathrm{d}W(z)}{\mathrm{d}z} \tag{33}$$

The "acceleration" of the chain $\mathrm{d}^2S^o(t)/\mathrm{d}t^2$ is zero along its entire length as it is uniformly stretched. The equation of motion simplifies in this approximation to

$$0 = \frac{\mathrm{d}V(z)}{\mathrm{d}z} + (1-2g(t))\frac{\mathrm{d}W(z)}{\mathrm{d}z} \tag{34}$$

We transform $g(t)$ into a function of z by recognizing that the constant "velocity" v of the uniformly stretched chain must be such that it spans L in N monomers

$$L = \int_0^N \mathrm{d}t\, v \tag{35}$$

Thus, the chain is simply a path in z given by

$$S^o(t) = vt = z(t) \tag{36}$$

where $v = (L/N)$. With this, $g(t)$ is written as a function of z by

$$g(z) = 1 - \frac{z}{L} = \phi_{\mathrm{A}}^o(z) \tag{37}$$

where this is just the sawtooth monomer concentration profile.

We are now in the position to obtain analytical expressions for $V(z)$, $W(z)$, and $U(z)$ in the strongly stretched limit. Starting with $W(z)$, we have

$$W^o(z) = \frac{1}{2}\chi\,(\phi_{\mathrm{A}}^o(z) - \phi_{\mathrm{B}}^o(z)) = \chi\left(\frac{1}{2} - \frac{z}{L}\right) \tag{38}$$

Next, $U(z)$ is given via eq 31 as

$$U^o(z) = -\frac{1}{4}\chi\,(\phi_{\mathrm{A}}^o(z) - \phi_{\mathrm{B}}^o(z))^2 = -\frac{\chi}{L^2}\left(z - \frac{L}{2}\right)^2 \tag{39}$$

Finally, we integrate eq 34 in z to obtain the analytical form of $V(z)$,

$$V^o(z) = \frac{1}{4}\chi\,(\phi_{\mathrm{A}}^o(z) - \phi_{\mathrm{B}}^o(z))^2 + C^o = \frac{\chi}{L^2}\left(z - \frac{L}{2}\right)^2 + C^o \tag{40}$$

The constant C^o uniformly shifts the hydrostatic pressure field, and is equal to the constant of integration minus $\chi/4$ so that the first term of the equation is a perfect square. (Recall that shifting $V(z)$ by an additive constant does not influence the physics of the problem.)

The net field acting on a single strongly stretched chain, $U^o(z) + V^o(z)$, sums to the constant C^o at all z as expected. This is quite different from the case of homopolymer brushes, in which the necessity for chain trajectories to reach the grafting surface from any starting point above it, via the same number of monomers (the "equal-time" constraint), gives rise to a net *parabolic* potential.[32] In contrast, for linear gradient copolymers, we argue that the strongly stretched limit is characterized by only uniformly stretched chains beginning at $z = 0$ and traveling to $z = L$ at constant velocity in N monomers. The net potential for the system must therefore be the constant C^o as found.

The free energy for a single chain in the uniformly stretched limit is obtained by

$$\frac{F_1^o}{k_{\mathrm{B}}T} = -\ln Z_1^o[V^o(z), W^o(z)] - \frac{N}{L}\int_0^L \mathrm{d}z\,[V^o(z) + U^o(z)] \tag{41}$$

The natural logarithm of Z_1^0, eq 32, is managed by transforming the segmental t integral into a positional z integral via eq 36. Then, substitution of eqs 37−40 into eqs 41 and the transformed 32 results in

$$\frac{F_1^o}{k_{\mathrm{B}}T} = \frac{3}{2a^2}\frac{L^2}{N} - \frac{1}{12}\chi N \tag{42}$$

The free energy per chain in the strongly stretched limit is equal to the stretch entropy of the chain plus half the interaction energy between the chain and the monomer concentration field.

Profiles of $V^o(m)$, $W^o(m)$, $U^o(m)$, and C^o are superimposed onto our numerical results in Figure 4 through Figure 7. The deviations of the actual fields from the strongly stretched limiting forms may be interpreted as relative measures of fluctuations from uniform stretching in the vicinity of m. The largest divergence from the ideal limit occurs near the edges of the profiles. This lessens when the chains are enthalpically driven toward full constant stretching as χN increases. In contrast, the midsections of the chains even at very low χN are constantly stretched. This leads to the notion that fluctuations occur predominantly at the chain ends.

Chain Conformations and Stretching. Using numerical self-consistent field results, we can also visualize the spatial probability distributions of individual segments for a single copolymer chain to more thoroughly consider where it deviates from the uniform-stretch limit.

It is tempting to obtain the distribution of segment n by plotting $p(m,n)$ over all lattice layers, 1 to M; however, $p(m,n)$ includes segment density contributions from the tails of chains beyond the two reflecting lattice boundaries. The segment distributions of just *one* chain are obtained by propagation of the random walkers in a lattice of width $3M$. This expanded lattice contains three periods of the $V^*(m)$ and $\phi_{\mathrm{A}}(m)$ profiles obtained from the self-consistent field methodology described earlier. (It is desirable that chain tail overlap is included when determining the forms of the fields themselves, as this is representative of what occurs in a real lamellar system.) The intermediate region from M to $2M$ contains V^* and ϕ_{A} as computed; the two adjacent regions from 1 to M and $2M$ to $3M$ contain mirror images of the two fields. Next, the condition that the chain begins and ends about M and $2M$, respectively, is imposed. The allowed starting and ending zones are chosen such that the probability distributions of segments $n = 1$ and N are not cut off until their values are two to 3 orders of magnitude below their maxima. This permits inclusion of only the chain conformations that travel from the vicinity of M to near $2M$ in the distribution of random walker pathways while discarding conformations that travel from M to 1 and $3M$ to $2M$. Note that this does not affect the conformational distribution of the single

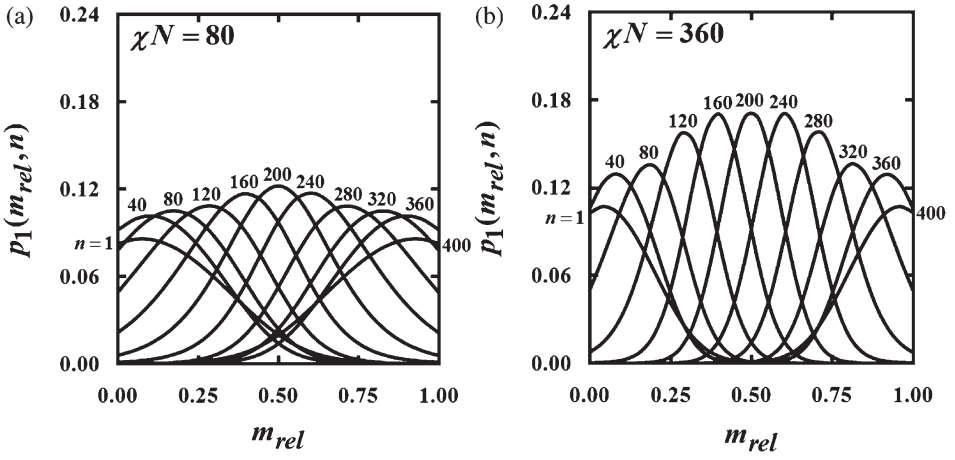

Figure 8. Concentration of selected segments $n = 1, 40, 80, ...$, along a single linear gradient copolymer chain in a melt lamella (see eq 43). Results for $\chi N = 80$ (a) and 360 (b).

chain in question; its pathway *only* depends upon the forms of the self-consistent fields obtained initially.

The sum of Boltzmann weights for chain trajectories where segment n is at layer m (in the expanded lattice of $3M$ layers), with overlap of segment distributions from other chains removed by the technique described above, is $Q_1(m,n)$. The spatial probability distribution for segment n is thus calculated by

$$p_1(m,n) = \frac{Q_1(m,n)}{\Sigma_{m=1}^{3M} Q_1(m,n)} \tag{43}$$

Plots of the distributions over the intermediate region M ($m_{rel} = 0$) to $2M$ ($m_{rel} = 1$) for a sequence of segments are shown in Figure 8 for $\chi N = 80$ (a) and $\chi N = 360$ (b). There is striking regularity in the peak location and width of each distribution for the chains' midsections; the chain conformations are evidently close to uniformly stretched. The terminal monomers of the chains, however, have far broader distributions, and display much weaker stretching (distributions for monomers 360 and 400, for example, are nearly coincident, even for $\chi N = 360$).

The segment distributions and self-consistent field profiles for linear gradient copolymer melt lamellae present compelling evidence for uniformly stretched chains with fluctuation corrections at the ends. In the next section, we shall construct a scaling theory that accounts for this behavior, and predicts the scaling of lamellar period with χN.

Scaling Theory

In the previous section, we argued that in the limit of strong segregation, the monomer concentration profile must tend to a sawtooth, with uniformly stretched chains. However, the argument that led to that conclusion was not sufficient to determine the lamellar period. In our numerical results, we observed that the concentration profile approached a sawtooth for strongly immiscible A−B interactions, with rounding of the "teeth" decreasing as χN increased. We now construct a scaling theory of the lamellar phase in linear gradient copolymers that accounts for the rounding of the concentration profile, and the scaling of the lamellar period.

Our scaling theory takes the form of a Flory approximation for the free energy per chain F_{chain} as the sum of two competing terms, one entropic, the other energetic, both depending on the lamellar period L_{eq}, which is to be found by minimizing F_{chain} with respect to L. The entropic term arises from chain stretching, and takes the customary form for Flory theories of $F_{stretch} = k_B T L^2/R_g^2$.[30]

As the lamellar period increases and chains become more stretched, fluctuations in the positions of monomers along the chains become smaller. The length scale for these fluctuations is the "tension blob" size ξ, which satisfies the usual scaling relations[30]

$$\begin{aligned} N/g &\sim L/\xi \\ \xi^2 &\sim g a^2 \end{aligned} \tag{44}$$

in which g is the number of monomers in a tension blob.

The first relation above expresses the fact that the stretched chain of length L may be regarded as a linear string of N/g stretch blobs, each of length ξ; the second indicates that within a stretch blob, the chain scales as a random walk. Together these relations yield that the tension blob size is set by the "stretch ratio" R_g/L as

$$\xi/L \sim R_g^2/L^2 \tag{45}$$

The size ξ of the tension blob sets the length scale for the positional fluctuation of monomers along the stretched chain, and hence the length scale for rounding of the sawtooth concentration profile.

The energetic term in our Flory theory F_{int} accounts for the increase in monomer interaction energy that results from the rounding of the sawtooth profile, which leads to a slightly less effective separation of A and B monomers than does the sharp sawtooth.

To estimate F_{int}, we argue as follows. First, we observe that for a chain segment located somewhere along a strictly linear monomer concentration profile, symmetric fluctuations in segment position z about some mean location $\langle z \rangle$ have zero effect on the average interaction energy of the segment with the concentration profile. (This results because the distribution of segment positions is an even function of $\delta z = z - \langle z \rangle$, while the variation of the concentration profile about z is an odd function of δz.) But at the ends of the concentration profile, i.e., at the tips of the sawteeth, fluctuations in the monomer positions smear the concentration profile over a distance ξ, flattening the teeth and thus reducing the concentration of the majority monomer.

We can most easily calculate the monomer interaction energy per chain by integrating the local monomer interaction over the entire lamella, and then dividing by the number of chains J in the system. We can write J conveniently as the ratio AL/Na^3, where Na^3 is the volume of a chain, and AL is the lamellar volume (A the lamellar area). Then we have

$$\begin{aligned} F_{\rm int} &= \frac{Na^3}{AL}\frac{1}{2} k_B T \chi \int d^3\mathbf{r} \frac{1}{a^3} \phi_A(\mathbf{r})(1-\phi_A(\mathbf{r})) \\ &= \frac{N}{L}\frac{1}{2} k_B T \chi \int_0^L dz\, \phi_A(z)(1-\phi_A(z)) \end{aligned} \tag{46}$$

Now the infinitely sharp sawtooth concentration profile $\phi_A^o(z)$ is perturbed by the rounding, as $\phi_A(z) = \phi_A^o(z) + \delta\phi_A(z)$, where

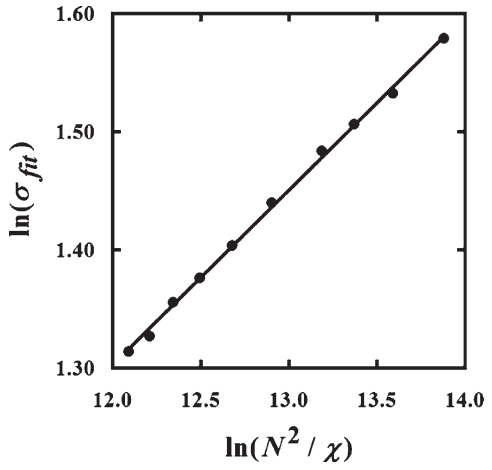

Figure 9. The log−log plot of $\ln(N^2/\chi)$ versus the standard deviation of the Gaussian curve fitted to the spatial probability distribution of chain segment 1, $\ln(\sigma_{fit})$. Solid line is linear fit, with slope 0.148 ± 0.002.

$\delta\phi_A(z)$ is of order $\pm\xi/L$ over a width ξ at the tip of the tooth (with opposite signs at the top and bottom of the sawtooth profile). Expanding F_{int} to first order in $\delta\phi_A$, we have

$$\Delta F_{\text{int}} = F_{\text{int}} - F^{o}_{\text{int}} = \frac{N}{L}\frac{1}{2} k_B T\chi \int_0^L \mathrm{d}z\, \delta\phi_A(z)(1-2\phi^{o}_A(z)) \sim k_B T\chi N\left(\frac{\xi}{L}\right)^2 \quad (47)$$

in which the final scaling results from using the appropriate scaling for $\delta\phi_A(z)$ and noting that $\phi^{o}_A(z)$ is nearly unity at the top tooth (and zero at the bottom).

Thus, our two-term Flory theory takes the form

$$F_{chain} = F_{stretch} + \Delta F_{\text{int}} = \frac{L^2}{{R_g}^2} + \chi N\left(\frac{R_g}{L}\right)^4 \quad (48)$$

in which we have inserted the scaling of the tension blob (and dropped inessential factors of k_BT). Minimizing with respect to L gives the scaling of the equilibrium lamellar period as

$$\frac{L_{eq}}{R_g} \sim (\chi N)^{1/6} \quad (49)$$

This result compares reasonably well with the fit exponent obtained from our self-consistent field calculations (eq 29). Remarkably, the scaling of the lamellar period for linear gradient copolymers turns out to be the same as for symmetric diblock copolymer melts,[25] although the physical origin of the scaling is quite different in the two cases.

We can check our scaling theory in another way by comparing the widths of the spatial probability distributions for a terminal monomer (we choose chain segment 1), to the size of the tension blob as a function of χN. Rearrangement of our scaling theory shows that the blob length ξ scales as

$$\xi \sim \left(\frac{N^2}{\chi}\right)^{1/6} \quad (50)$$

Thus, a log−log plot of the distribution width for the end segment versus N^2/χ should display a power law of 1/6. We determine the distribution width from our numerical results by fitting each distribution to a Gaussian of the form

$$p_{fit}(m, n = 1) = \frac{1}{\sqrt{2\pi}\sigma_{fit}} \exp\left[-\frac{(m-\overline{m})}{2{\sigma_{fit}}^2}\right] \quad (51)$$

from which a fitted standard deviation, σ_{fit}, is obtained. This fit is independently performed for the distribution of segment 1, $p_1(m, n = 1)$, for every χN studied. The distributions are quite well described by Gaussians; the fit error relative to each σ_{fit} averages to 0.26%. Figure 9 is a plot of $\ln(N^2/\chi)$ against $\ln(\sigma_{fit})$. A least-squares fit of the log−log points gives

$$\sigma_{fit} \sim \left(\frac{N^2}{\chi}\right)^{0.148 \pm 0.002} \quad (52)$$

in good agreement with our scaling theory, eq 50.

Conclusions

We have investigated the equilibrium self-assembly of linear gradient copolymer lamellar phases, using both numerical solutions of self-consistent field equations, as well as analytical theory and scaling arguments.

For the numerical work, we have used the lattice formulation of self-consistent field theory developed by Scheutjens and Fleer, and applied previously by Lefevbre et al.[19] to gradient copolymer lamellae. We have extended their results to look more closely at the dependence on χN of the composition and self-consistent field profiles, as well as the conformations of individual copolymer chains, in order to understand the strong segregation regime for this new chain architecture.

We find that the nearly sinusoidal concentration profiles observed for linear gradient copolymer lamellae at moderate χN values progressively sharpen toward a "sawtooth" profile as χN increases. We argue that in the strong-segregation limit, in which the repulsive energetic interaction between A and B monomers is dominant, the chain conformations should become uniformly stretched, so that portions of a chain with a given average concentration will be surrounded by other chain segments with exactly the same average concentration. We directly observe this state of nearly uniform stretching in our numerical mean-field results, applied to the conformations of single chains.

The above argument however does not determine the lamellar period L, since chains precisely stretched to any length L would satisfy the same requirement. To predict the lamellar period, we must account as well for the effect of fluctuations around the uniformly stretched limiting state. This we do by means of a Flory theory, which balances the entropy cost of chain stretching with the increase in A−B monomer interactions that result when monomer positional fluctuations lead to smearing of the concentration profile near the tips of the sawteeth. (The length scale for the smearing is the size of a tension blob, which scales with the "stretch ratio" L/R_g in the usual way, $\xi/L \sim (R_g/L)^2$.)

The result of our scaling analysis is that L_{eq}/R_g scales as $(\chi N)^{1/6}$, which is in good agreement with our numerical results for the equilibrium lamellar period. The length scale of the end segment distributions is likewise consistent with the implied scaling of ξ, as $(N^2/\chi)^{1/6}$.

Remarkably, the scaling of lamellar period with χN we find for linear gradient copolymers has the same exponent as for the case of symmetric diblock lamellae. However, the physics of self-assembly in the two cases are very different. For the linear gradient copolymers, the varying composition of the chains gives rise to an A-B monomer interaction field that drives the A-rich and B-rich ends of the chains away from the relatively broad region where the chain center monomers reside. This is balanced by the hydrostatic pressure field that draws the chains inward, to enforce constant melt density. In contrast, the A-B monomer interaction field in symmetric diblock copolymer lamellae results in localization of the chain junction points on a relatively narrow interface. The hydrostatic pressure field then pushes the chains outward from the interface.

We also construct the strong-segregation limit for the most-probable conformation of a single linear gradient copolymer chain in the self-consistent potentials, and the corresponding strong-segregation limiting forms for those potentials. These results are analogous to the "classical" or "strong-stretching" limit for grafted polymer brushes, but quite different in detail, in that the limiting trajectory for linear gradient copolymers is indeed uniformly stretched. Our numerical results for the spatial dependence of the self-consistent chemical potential and pressure fields are consistent with our analytical strong-segregation predictions.

As for grafted polymer brushes and strongly segregated diblock copolymer mesophases, the availability of convenient analytical results for the self-assembled structures formed by linear gradient copolymers should be useful in designing and predicting the properties of these promising new materials.

Acknowledgment. Financial support provided by the National Science Foundation (DMR-0804593 to J.E.G.L. and DMR-0851897 to S.T.M.) and the Petroleum Research Fund to STM (49964-ND7) is gratefully acknowledged.

Appendix A. Monomer Interaction Expression

The form of $W^*(m)(1 - 2g(n))$, i.e. eq 18, can also be arrived at by considering the chemical potential for the replacement of monomer type $1 - g(n)$ with a monomer of type $g(n)$ in a local "sea" of A/B monomers with composition $\phi_A(m)$. This problem is approached by treating layer m as its own self-contained incompressible Flory−Huggins (FH) lattice. The energy of mixing in the lattice follows the standard FH solution theory

$$\frac{\Delta E}{k_B T} = \chi r_A(m)\left(\frac{r_B(m)}{r}\right) \tag{53}$$

where r_i is the number of i-type monomers on the FH lattice of r sites. The lattice is incompressible, so it follows that $r_B = r - r_A$. The exchange chemical potential for a type A monomer in the lattice is half the change in internal energy upon inserting an A monomer and removing a B monomer. It is given by

$$\frac{1}{2}\left[\frac{\partial(\Delta E/k_B T)}{\partial r_A} - \frac{\partial(\Delta E/k_B T)}{\partial r_B}\right] = \frac{\mu_A}{k_B T}$$
$$= \frac{1}{2}\chi\,(\phi_B(m) - \phi_A(m)) \tag{54}$$

noting that $\partial r/\partial r_i = 1$ for $i = A$ and B. A similar expression is also valid for the exchange chemical potential of species B,

$$\frac{1}{2}\left[\frac{\partial(\Delta E/k_B T)}{\partial r_B} - \frac{\partial(\Delta E/k_B T)}{\partial r_A}\right] = \frac{\mu_B}{k_B T}$$
$$= \frac{1}{2}\chi\,(\phi_A(m) - \phi_B(m)) \tag{55}$$

which is just W^*. The key, now, is to determine the chemical potential for species $g(n)$. This is written by scalar multiples of the pure A and B exchange potentials as

$$\frac{\mu_{g(n)}}{k_B T} = g(n)\,\frac{\mu_A}{k_B T} + (1 - g(n))\,\frac{\mu_B}{k_B T} \tag{56}$$

Substitution of the two pure exchange potential expressions above yields, upon simplification,

$$\frac{\mu_{g(n)}}{k_B T} = \frac{1}{2}\chi\,(\phi_A(m) - \phi_B(m))(1 - 2g(n)) \tag{57}$$

This is precisely the expression for the local interaction of segment n with the environment at layer m, eq 18, as obtained from the partition function subjected to self-consistency.

References and Notes

(1) Matyjaszewski, K.; Tsarevsky, N. V. *Nature Chem.* **2009**, *1*, 276.
(2) Moad, G.; Rizzardo, E.; Thang, S. H. *Polymer* **2008**, *49*, 1079.
(3) Hawker, C. J.; Bosman, A. W.; Harth, E. *Chem. Rev.* **2001**, *101*, 3661.
(4) Beginn, U. *Colloid Polym. Sci.* **2008**, *286*, 1465.
(5) Amirova, L. M.; Andrianova, K. A. *J. Appl. Polym. Sci.* **2006**, *102*, 96.
(6) Kim, J.; Mok, M. M.; Sandoval, R. W.; Woo, D. J.; Torkelson, J. M. *Macromolecules* **2006**, *39*, 6152.
(7) Karaky, K.; Billon, L.; Pouchan, C.; Desbrires, J. *Macromolecules* **2007**, *40*, 458.
(8) Jakubowski, W.; Juhari, A.; Best, A.; Koynov, K.; Pakula, T.; Matyjaszewski, K. *Polymer* **2008**, *49*, 1567.
(9) Mok, M. M.; Pujari, S.; Burghardt, W. R.; Dettmer, C. M.; Nguyen, S. T.; Ellison, C. J.; Torkelson, J. M. *Macromolecules* **2008**, *41*, 5818.
(10) Sun, X.; Luo, Y.; Wang, R.; Li, B.-G.; Zhu, S. *AIChE J.* **2008**, *54*, 1073.
(11) Mok, M. M.; Kim, J.; Wong, C. L. H.; Marrou, S. R.; Woo, D. J.; Dettmer, C. M.; Nguyen, S. T.; Ellison, C. J.; Shull, K. R.; Torkelson, J. M. *Macromolecules* **2009**, *42*, 7863.
(12) Bates, F. S.; Fredrickson, G. H. *Phys. Today* **1999**, *52*, 32.
(13) Matsen, M. W. *J. Phys.: Condens. Matter* **2002**, *14*, R21.
(14) Park, C.; Yoon, J.; Thomas, E. L. *Polymer* **2003**, *44*, 6725.
(15) Fredrickson, G. H. *The Equilibrium Theory of Inhomogeneous Polymers*; Oxford University Press: New York, 2006.
(16) Andelman, D.; Rosensweig, R. E. *J. Phys. Chem. B* **2009**, *113*, 3785.
(17) Pakula, T.; Matyjaszewski, K. *Macromol. Theory Simul.* **1996**, *5*, 987.
(18) Aksimentiev, A.; Holyst, R. *J. Chem. Phys.* **1999**, *111*, 2329.
(19) Lefebvre, M. D.; de la Cruz, M. O.; Shull, K. R. *Macromolecules* **2004**, *37*, 1118.
(20) Jiang, R.; Jin, Q.; Li, B.; Ding, D.; Wickham, R. A.; Shi, A.-C. *Macromolecules* **2008**, *41*, 5457.
(21) Wang, R.; Li, W.; Luo, Y.; Li, B.-G.; Shi, A.-C.; Zhu, S. *Macromolecules* **2009**, *42*, 2275.
(22) Shull, K. R. *Macromolecules* **2002**, *22*, 8631.
(23) Pickett, G. T. *J. Chem. Phys.* **2003**, *118*, 3898.
(24) Helfand, E. *Macromolecules* **1975**, *8*, 552.
(25) Helfand, E.; Wasserman, Z. R. *Macromolecules* **1976**, *9*, 879.
(26) Shull, K. R. *Macromolecules* **1992**, *25*, 2122.
(27) Scheutjens, J. M. H. M.; Fleer, G. J. *J. Phys. Chem.* **1979**, *83*, 1619.
(28) Scheutjens, J. M. H. M.; Fleer, G. J. *J. Phys. Chem.* **1980**, *84*, 178.
(29) Lefebvre et al.[19] define L as the width of one full lamellar period, equal to the width of two lamellae.We instead choose to define L as half the width of a lamellar period, the width of just one lamella, for clearer presentation of numerical results and more symmetric mathematical forms of our strong-stretching theory.
(30) de Gennes, P.-G. *Scaling Concepts in Polymer Physics*; Cornell University Press: Ithaca, New York, 1979.
(31) Edwards, S. F. *Proc. Phys. Soc. London* **1965**, *85*, 613.
(32) Milner, S. T. J. *Polym. Sci., Part B: Polym. Phys.* **1994**, *32*, 2743.